

## Exact dipole solitary wave solution in metamaterials with higher-order dispersion

Xuemin Min, Rongcao Yang, Jinping Tian, Wenrui Xue & J. M. Christian

To cite this article: Xuemin Min, Rongcao Yang, Jinping Tian, Wenrui Xue & J. M. Christian (2016): Exact dipole solitary wave solution in metamaterials with higher-order dispersion, Journal of Modern Optics, DOI: [10.1080/09500340.2016.1185178](https://doi.org/10.1080/09500340.2016.1185178)

To link to this article: <http://dx.doi.org/10.1080/09500340.2016.1185178>



© 2016 The Author(s). Published by Informa UK Limited, trading as Taylor & Francis Group.



Published online: 17 May 2016.



Submit your article to this journal [↗](#)



Article views: 132



View related articles [↗](#)



View Crossmark data [↗](#)

# Exact dipole solitary wave solution in metamaterials with higher-order dispersion

Xuemin Min<sup>a</sup>, Rongcao Yang<sup>a</sup>, Jinping Tian<sup>a</sup>, Wenrui Xue<sup>a</sup> and J. M. Christian<sup>b</sup>

<sup>a</sup>College of Physics & Electronics Engineering, Shanxi University, Taiyuan, China; <sup>b</sup>Joule Physics Laboratory, Materials & Physics Research Group, School of Computing, Science and Engineering, University of Salford, Greater Manchester, UK

## ABSTRACT

We present an exact dipole solitary wave solution in a mutual modulation form of bright and dark solitons for a higher-order nonlinear Schrödinger equation with third- and fourth-order dispersion in metamaterials (MMs) using an ansatz method. Based on the Drude model, the formation conditions, existence regions and propagation properties are discussed. The results reveal that the solitary wave may exist in a few parameter regions of MMs, different from those in optical fibres, and its propagation properties can be controlled by adjusting the frequency of incident waves in each existence region.

## ARTICLE HISTORY

Received 30 November 2015  
Accepted 26 April 2016

## KEYWORDS

Dipole solitary wave;  
higher-order dispersion;  
metamaterials


## 1. Introduction

Solitons are regarded as ideal information carriers in optical communication systems due to their properties of keeping their shapes during propagation (1, 2). In fibre optics, solitons have been extensively studied in theory and experiments (3–5). Families of nonlinear Schrödinger equations (NLSEs) are well-known models for studying soliton propagation from different viewpoints. Seeking new exact soliton solutions for various generalized NLSEs remains a highly active research topic in the literature. For example, efficient ansatz approaches have been used to derive various exact solitons, including bright, dark and combined solitary wave solutions (6–15). In particular, new types of combined solitary wave solutions for several higher-order NLSEs (HNLSEs) have been reported, obtained using an ansatz comprising the *sum* of bright and dark solitary waves (9–12). Another interesting ansatz, involving the *product* of bright and dark solitary waves, has also been adopted to describe the propagation of dark-type optical pulses with finite width background (13). Related solutions, such as the so-called dark-in-the-bright and dipole solitons, are now known for HNLSEs with non-Kerr nonlinearity and third-order dispersion (TOD) (14, 15).

Alongside optical fibres research, metamaterials (MMs) attract considerable interest due to their unique and

technologically exploitable electromagnetic properties. Many potential applications have been proposed in the fields of applied electromagnetism and optics, including superlenses, invisibility cloaks and omnidirectional filters. Most recently, much attention has been paid to ultrashort pulse propagation in MMs (16–29) with theoretical models establishing (16–19) that dispersive permeability plays an important role in the formation of solitary waves. The existences of bright and dark gap solitons supported by negative-index MMs have also been predicted. Moreover, bright, dark (grey), combined and chirped solitary wave solutions of generalized NLSEs with higher-order nonlinear effects in MMs have been derived (24–29). To the best of our knowledge, dipole solutions for MMs have not yet been investigated.

In this paper, we investigate a generalized NLSE relevant to MMs with Kerr nonlinearity and higher-order dispersion. An exact dipole solitary wave solution is found from an ansatz method, and the formation conditions and existence regions are discussed in the context of the Drude model. Our results show that MM dipole solutions are markedly different from those in optical fibres. For instance, they can exist in a few regions of parameter space where the higher-order dispersion is not completely compensated, and the solitary wave properties are adjustable by tuning the frequency of incident waves.

**CONTACT** Rongcao Yang  sxdxyrc@sxu.edu.cn

© 2016 The Author(s). Published by Informa UK Limited, trading as Taylor & Francis Group.

This is an Open Access article distributed under the terms of the Creative Commons Attribution-NonCommercial-NoDerivatives License (<http://creativecommons.org/licenses/by-nc-nd/4.0/>), which permits non-commercial re-use, distribution, and reproduction in any medium, provided the original work is properly cited, and is not altered, transformed, or built upon in any way.

## 2. Theoretical model and dipole solitary wave solution

In homogeneous nonlinear MMs, the propagation of ultrashort pulses can be described by a HNLSE with TOD, a cubic-quintic nonlinearity and self-steepening (SS) (17–19). As the pulses become narrower in time, fourth-order dispersion (FOD) should also be taken into account. The theoretical model of ultrashort pulse propagation in MMs can then be written as (17–19).

$$\frac{\partial E}{\partial Z} = -\frac{i\beta_2}{2} \frac{\partial^2 E}{\partial T^2} + \frac{\beta_3}{6} \frac{\partial^3 E}{\partial T^3} + \frac{i\beta_4}{24} \frac{\partial^4 E}{\partial T^4} + i\gamma_0 \left[ |E|^2 E - \sigma |E|^4 E + is_1 \frac{\partial}{\partial T} (|E|^2 E) \right], \quad (1)$$

where  $E(Z, T)$  is the complex envelope of the electric field,  $Z$  and  $T$  represent the propagation distance and time in a retarded frame. The parameters  $\gamma_0 = \omega_0^2 \epsilon_0 \chi^{(3)} \mu(\omega_0) / (2k_0)$  and  $\sigma = \gamma_0 / (2k_0)$  describe the Kerr and pseudo-quintic nonlinearities, respectively, while  $s_1 = 1/\omega_0 - 1/(k_0 v_g) + \partial[\omega\mu(\omega)]/(\partial\omega)/[\omega\mu(\omega)]|_{\omega=\omega_0}$  controls the SS effect. Group-velocity dispersion (GVD), TOD and FOD are described by  $\beta_2 = \delta_2 - 1/(k_0 v_g^2)$ ,  $\beta_3 = \delta_3 + 3\beta_2/(k_0 v_g)$ , and  $\beta_4 = \delta_4 - 3\beta_2^2/k_0$ , respectively, where  $\delta_m = m! \sum_{l=0}^m F_l G_{m-l} / (2k_0)$ ,  $F_m = \partial^m[\omega\epsilon(\omega)] / (m! \partial\omega^m)|_{\omega=\omega_0}$  and  $G_m = \partial^m[\omega\mu(\omega)] / (m! \partial\omega^m)|_{\omega=\omega_0}$ . The dispersive permittivity and permeability of the MM are determined by  $\epsilon(\omega)$  and  $\mu(\omega)$ , respectively,  $v_g = 2k_0 / (F_0 G_1 + F_1 G_0)$  is the group velocity of the pulse,  $k_0 = n(\omega_0) \omega_0 / c$  is the wavenumber and  $n(\omega_0) = \pm \sqrt{\epsilon(\omega_0) \mu(\omega_0)}$  is the refractive index of medium at the carrier frequency  $\omega_0$ .

It should be noted that Equation (1) has the same form as the model for ultrashort pulse propagation in fibres (1). However, the two are of different physical significance, which stems from the distinct electromagnetic characteristics of MMs and fibres. The former has a dispersive permeability and a potentially negative refractive index, while the latter has a constant permeability and exhibits only positive refraction. Hence, the coefficients parameterizing Equation (1) are directly related to the magnetic properties of the system. It has been demonstrated that dispersive permeability plays a key role in the propagation of pulses in MMs (17–27). For instance, the pseudo-quintic term may enhance the cubic nonlinear response in MMs, whereas it typically weakens the cubic nonlinearity in fibres. The SS effect is also different in MM and fibre contexts: while the trailing edge of a pulse tends to steepen

in fibres, one may encounter steepening at either the leading or trailing edges in MMs. Therefore, it is necessary to investigate the formation and propagation of various solitons in MMs.

For weak nonlinearity and instantaneous MMs, the SS and the quintic contributions may be neglected. Thus, Equation (1) may be simplified to the following normalized form:

$$\frac{\partial U}{\partial \zeta} = -\frac{ib_2}{2} \frac{\partial^2 U}{\partial \tau^2} + \frac{b_3}{6} \frac{\partial^3 U}{\partial \tau^3} + \frac{ib_4}{24} \frac{\partial^4 U}{\partial \tau^4} + ib_1 |U|^2 U. \quad (2)$$

Here,  $U = E/E_0$ ,  $\zeta = Z/L_D$  and  $\tau = T/T_0$  are the normalized electric field amplitude, propagation distance and time, respectively, where  $L_D = T_0^2/|\beta_2|$  is the dispersion length and  $T_0$  is the initial duration of pulse. The parameter  $b_2 = \text{sgn}[\beta_2] = \pm 1$  stands for normal- or anomalous-GVD, while  $b_3 = \beta_3/|\beta_2|T_0$  and  $b_4 = \beta_4/|\beta_2|T_0^2$  parameterize TOD and FOD, respectively. The nonlinearity coefficient is  $b_1 = \theta N^2$ , where  $\theta = \text{sgn}[\gamma_0] = \pm 1$  corresponds to the self-focusing or self-defocusing nonlinearity and  $N$  is the order of solitons. In MMs, the dispersive dielectric permittivity and magnetic permeability are usually described by the Drude model  $\epsilon(\omega) = \epsilon_0 \left[ 1 - \omega_{pe}^2 / (\omega(\omega + i\gamma_e)) \right]$  and  $\mu(\omega) = \mu_0 \left[ 1 - \omega_{pm}^2 / (\omega(\omega + i\gamma_m)) \right]$  (19), where  $\omega_{pe}$  and  $\omega_{pm}$  are the respective electric and magnetic plasma frequencies, while  $\gamma_e$  and  $\gamma_m$  quantify the electric and magnetic losses. It should be pointed out that losses in MMs (which originate from the intrinsic absorption, scattering and the resonant nature of the magnetic response) are inevitably important (17, 30). However, measures can be taken to reduce or compensate dissipation, such as improving fabrication methods, introducing materials with optical gain and using optical parametric amplification (30–32). For simplicity, we neglect the role of losses in the following discussion. Accordingly, the coefficients in Equation (2) can now be simplified to  $\beta_2 = \beta / c n \omega_{pe} \varpi$ ,  $\beta_3 = -[2\gamma + 3(1 - \gamma/6)\beta/n^2] / c \omega_{pe}^2 \varpi^2 n$ ,  $\beta_4 = [10\gamma - 3\beta^2/n^2] / c \omega_{pe}^3 \varpi^3 n$ ,  $\gamma_0 = \chi^{(3)} \omega_{pe} \varpi (1 - \omega_p^2 \varpi^{-2}) / 2nc$ ,  $b_3 = \text{sgn}[\beta_3] s \left| -2\gamma/\beta - 3(1 - \gamma/6)/n^2 \right|$ ,  $b_4 = \text{sgn}[\beta_4] s^2 \left| 10\gamma/\beta - 3\beta/n^2 \right|$ , where  $\varpi = \omega_0 / \omega_{pe}$ ,  $\omega_p = \omega_{pm} / \omega_{pe}$ ,  $\gamma = 6\omega_{pe}^2 \omega_{pm}^2 / \omega_0^4$ ,  $\beta = (1 + \gamma/2) - (1 - \gamma/6)^2 / n^2$  and  $s = 1/\omega_0 T_0$ . As all the coefficients (except for  $\gamma_0$ ) are independent of nonlinearity, it follows that  $n$ ,  $\beta_2$ ,  $b_3$  and  $b_4$  in self-focusing

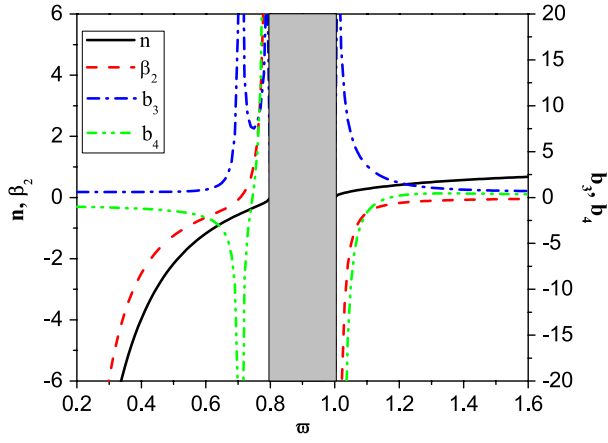


**Figure 1.** Curves of  $n$ ,  $\beta_2$ ,  $b_3$  and  $b_4$  vs.  $\omega$  in self-focusing MMs for  $\omega_p = 0.8$ , here  $\beta_2$  in units of  $10/c\omega_{pe}$ .

MMs are the same as those in self-defocusing MMs. The dependencies of these four key parameters on  $\omega$  are presented in Figure 1 for  $\omega_p = 0.8$ ,  $\omega_{pe} = 1.3673 \times 10^{16}$  Hz,  $\chi^{(3)} = 10^{-10}$  esu,  $T_0 = 50$  fs and  $s = 0.2$ . On the one hand, it is clear that  $\beta_2$  and  $b_4$  can be either positive or negative in the negative-index region ( $\omega < 0.8$ ), and they are always negative in the positive-index region ( $\omega > 1.0$ ). On the other hand,  $b_3$  is always positive in both negative- and positive-index regions. As mentioned in Refs. (17–19), the model coefficients directly related to  $\varepsilon(\omega)$  and  $\mu(\omega)$  can be tailored by engineering the unit-cell structure of MMs, which implies more possibilities for the existence of wider classes of solitary wave (17).

To seek dipole solitary waves of Equation (2), we adopt an ansatz of the form (13–15):

$$U(\zeta, \tau) = \lambda \tanh[\eta(\tau - \chi\zeta)] \operatorname{sech}[\xi(\tau - \chi\zeta)] e^{i(\kappa\zeta - \Omega\tau)}, \quad (3)$$

where  $\lambda$ ,  $\Omega$ ,  $\chi$  and  $\kappa$  represent the amplitude, frequency shift, inverse group velocity and wavenumber of the solution, respectively.  $\eta$  and  $\xi$  are related to the inverse pulse widths of the dark and bright components of the dipole. The intensity of solitary wave (3) is in the form  $|U(\zeta, \tau)|^2 = \lambda^2 \tanh^2[\eta(\tau - \chi\zeta)] \operatorname{sech}^2[\xi(\tau - \chi\zeta)]$ . Substituting Equation (3) into (2) and setting the coefficients of independent terms equal to zero, we can obtain a set of compatible equations. By solving these equations, we find Equation (2) has the solitary wave solution as follows:

$$U(\zeta, \tau) = \eta^2 \sqrt{5b_4/b_1} \tanh[\eta(\tau - \chi\zeta)] \operatorname{sech}[\eta(\tau - \chi\zeta)] e^{i(\kappa\zeta + b_3\tau/b_4)}, \quad (4)$$

with

$$\eta = \sqrt{3(b_3^2 - 2b_2b_4)/5b_4^2}, \quad (5a)$$

$$\chi = b_3(b_3^2 - 3b_2b_4)/3b_4^2, \quad (5b)$$

$$\kappa = (2b_3^4 - 8b_2b_3^2b_4 + 33b_2^2b_4^2)/50b_4^3. \quad (5c)$$

Dipole solitary wave (4) is an inter-modulation of bright and dark components with the same pulse width and velocity. Its intensity is  $|U(\zeta, \tau)|^2 = 5\eta^4 b_4/b_1 \tanh^2[\eta(\tau - \chi\zeta)] \operatorname{sech}^2[\eta(\tau - \chi\zeta)]$ , exhibiting a characteristic M-shape or dipole-type intensity distribution. It can be seen from Equations (4) and (5a) that the conditions  $b_1b_4 > 0$  and  $b_3^2 - 2b_2b_4 > 0$  must always be satisfied, which means that the formation of the solitary wave depends strongly upon different combinations of dispersion and nonlinearity. Moreover, the solution parameters  $\eta$ ,  $\Omega$ ,  $\chi$  and  $\kappa$  depend only on the dispersive properties embodied by  $b_2$ ,  $b_3$  and  $b_4$  and are independent of the nonlinearity [ $b_1$  influences only the existence regions of the solitary wave (4)]. By combining Figure 1 with the existence conditions, it is easy to show that when TOD and FOD are neglected, there are no regions of parameter space for either self-focusing or self-defocusing nonlinear MMs wherein dipole solitary wave (4) may reside. For finite higher-order dispersion, we find the solution can exist: (i) in the normal-GVD regime of self-focusing negative-index MMs and (ii) in all dispersion regimes of self-defocusing positive- and negative-index MMs. Table 1 shows the existence regions of solution (4) with the corresponding normalized frequency ranges in self-focusing and self-defocusing MMs. It can clearly be seen that the existence regions are quite different from those of bright or dark solitary waves in MMs (26, 27). Moreover, when compared with similar solutions in conventional materials (13–15), the MM dipole solitary wave may exist in additional regions of parameter space. A further distinction is that solution (4) in different existence regions possesses different parameters  $\eta$ ,  $\chi$ ,  $\Omega$  and  $\kappa$  because the model parameters  $b_2$ ,  $b_3$  and  $b_4$  in Equation (2) vary with the normalized frequency  $\omega$ . Figure 2 illustrates variations of parameters  $\eta$ ,  $\chi$ ,  $\Omega$  and  $\kappa$  with  $\omega$  in different existence regions. By comparing the plots in Figure 2, it is easy to see that in all allowed regions, the

**Table 1.** Existence regions of the solitary wave (4) in self-focusing and self-defocusing MMs.

	$b_1 = \operatorname{sgn}[\gamma_0]$	$b_2 = \operatorname{sgn}[\beta_2]$	Existence regions and $\omega$ ranges
I	1	1	$\omega \in [0.746, 0.799]$ $n < 0$
II	-1	-1	$\omega \in [0.677, 0.745]$ $n < 0$
III	-1	-1	$\omega \in [1.000, 1.171]$ $n > 0$

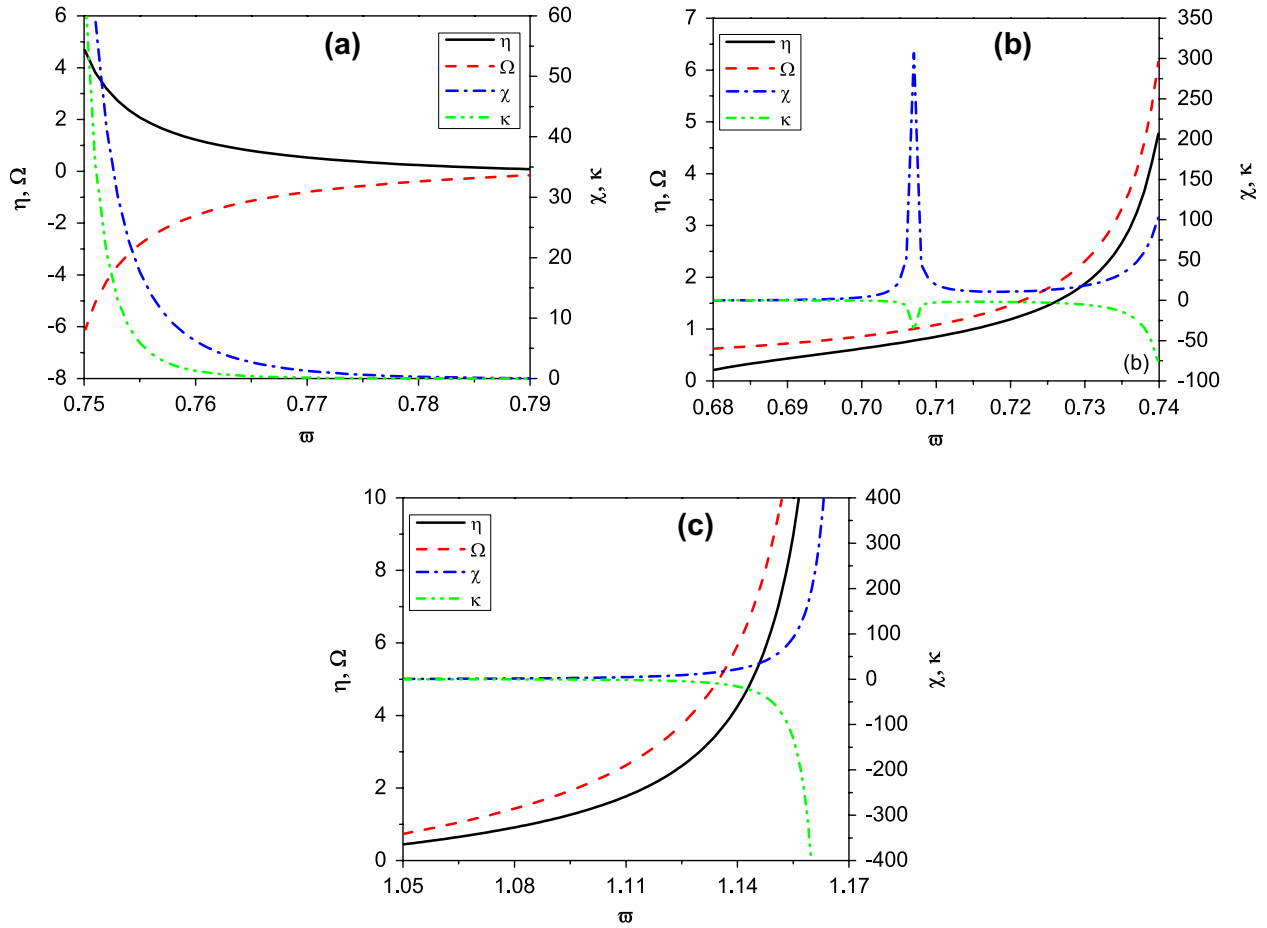


**Figure 2.** Curves of the parameters  $\eta$ ,  $\Omega$ ,  $\chi$  and  $\kappa$  of the solitary wave (4) vs.  $\varpi$  in (a) normal-GVD regime of self-focusing negative-index MMs; in (b) negative- and (c) positive-index regions of self-defocusing MMs, respectively.

frequency shift  $\Omega$  increases with  $\varpi$  while the wavenumber  $\kappa$  decreases. However, the behaviour of the inverse pulse width  $\eta$  and the inverse wave velocity  $\chi$  with  $\varpi$  is nearly opposite in self-focusing and self-defocusing nonlinear MMs. Conversely, as  $\varpi$  increases, both  $\eta$  and  $\chi$  decrease in self-focusing negative-index MMs [see Figure 2(a)] while they increase in both negative- and positive-index regions of self-defocusing MMs [see Figures 2(b) and (c)]. This means that we can control the properties of dipole solitary waves in self-focusing and self-defocusing nonlinear MMs by changing the frequency of incident waves.

It should be noted that  $\chi$  and  $\kappa$  in Figure 2(b) exhibit resonance-type behaviour at  $\varpi = 0.707$ . The reason for this behaviour is that in the negative-index regime, frequency  $\varpi = 0.707$  corresponds to the zero-GVD point (where  $\beta_2$  crosses from being negative to positive). The higher-order dispersion parameters  $b_3 = \beta_3/|\beta_2|T_0$  and  $b_4 = \beta_4/|\beta_2|T_0^2$  are then strongly peaked at that point, as shown in Figure 1. According to Equations (5a–c), the special case of  $b_2 = 0$  solution (4) has the following parameters:  $\lambda^2 = 9b_3^4/5b_1b_4^3$ ,  $\eta^2 = 3b_3^2/5b_4^2$ ,  $\Omega = -b_3/b_4$ ,

$\chi = b_3^3/3b_4^2$  and  $\kappa = b_4^4/25b_3^3$ . This means that the balance between TOD, FOD and Kerr nonlinearity can support the formation of a dipole solitary wave in self-defocusing MMs when the GVD is compensated.

Figure 3 presents a set of simulations showing the evolution of dipole solitary wave (4) in different existence regions for fixed  $\varpi$ . Here, we take the following parameter values in Figure 3(a) normal-GVD regime of self-focusing negative-index MMs,  $b_1 = 1$ ,  $b_2 = 1$  and  $\varpi = 0.766$  corresponding to  $b_3 = 8.962$  and  $b_4 = 8.429$ ; (b) anomalous-GVD regime of self-defocusing negative-index MMs,  $b_1 = -1$ ,  $b_2 = -1$  and  $\varpi = 0.678$  corresponding to  $b_3 = 3.629$  and  $b_4 = -5.967$ ; (c) normal-GVD regime of self-defocusing negative-index MMs,  $b_1 = -1$ ,  $b_2 = 1$  and  $\varpi = 0.713$  corresponding to  $b_3 = 25.083$  and  $b_4 = -21.413$ ; (d) anomalous-GVD regime of self-defocusing positive-index MMs,  $b_1 = -1$ ,  $b_2 = -1$  and  $\varpi = 1.070$  corresponding to  $b_3 = 4.975$ ,  $b_4 = -4.263$ . It should be pointed out that all adopted model parameters satisfy the existence conditions,

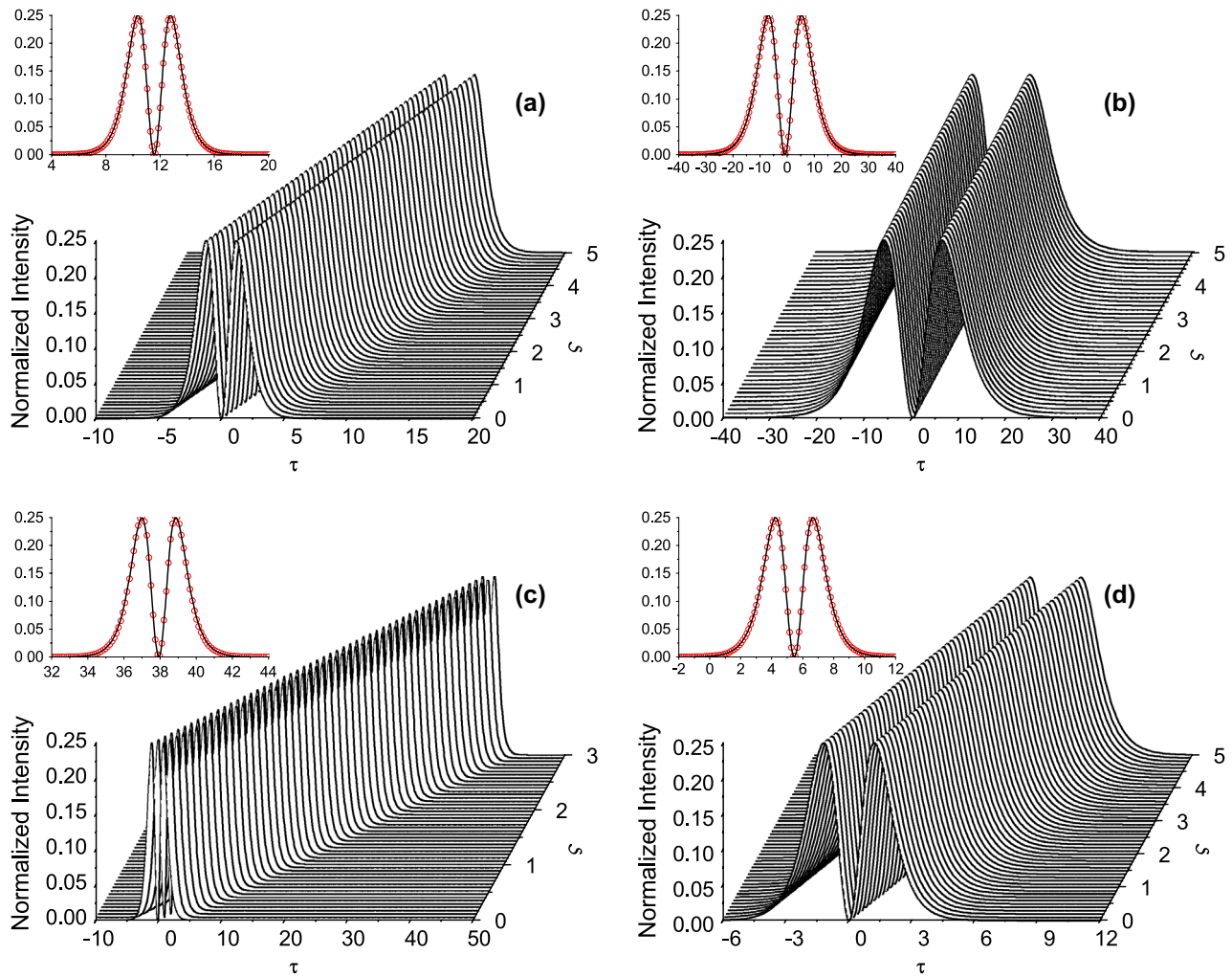


**Figure 3.** Evolutions of the solitary waves (4) (a) in normal-GVD regime of self-focusing negative-index MMs; in (b) anomalous- and (c) normal-GVD regimes of self-defocusing negative-index MMs; (d) in anomalous-GVD regime of self-defocusing positive-index MMs. Here, the intensities of the solitary wave are normalized by  $|U|^2/\lambda^2$ , and the corresponding  $b_3$  and  $b_4$  are shown in the text. Numerical confirmations (red circles) of the exact solutions (black solid line) are shown in the insets, respectively.

and the corresponding normalized frequencies are located in the existence ranges shown in Table 1. All the amplitudes of the solitary waves remain at the same value of 0.25 in Figure 3 because of the normalization  $|U|^2 \rightarrow |U|^2/\lambda^2$ . It can also be seen from Figure 3 that in different existence regions, the solitary waves have different pulse widths and velocities for fixed  $\omega$ , which are in agreement with the curves of Figure 2. The results show that mutual balancing between Kerr nonlinearity, GVD, TOD and FOD gives rise to the formation of the dipole solitary wave. In particular, the Kerr effect only influences the existence regions, while dispersion not only plays a role in the existence regions, but also influences the characteristics of propagating solitary waves. All the analytical predictions are verified by numerical simulations in each case, as shown in the insets.

Finally, we consider the stability of dipole solitary waves under perturbations. As examples, we investigate numerically the propagation of dipole solitary waves in the normal-GVD regime of self-focusing negative-index MMs and in the anomalous-GVD regime of self-defocusing negative-index MMs. It can be seen from Figures 4(a) and (b) that under 5% pulse width fluctuation, the solitary waves remain stable after propagating over 20 dispersion lengths. Under 10% of random noise perturbation, the dipole solitary waves in these two existence regions can still keep their initial shapes after propagating over 20 dispersion lengths except for a small deviation around the bipolar peaks and the backgrounds, as shown in Figures 4(c) and (d). The detailed stability analysis for the dipole solitary waves in all existence regions is now under further investigation.

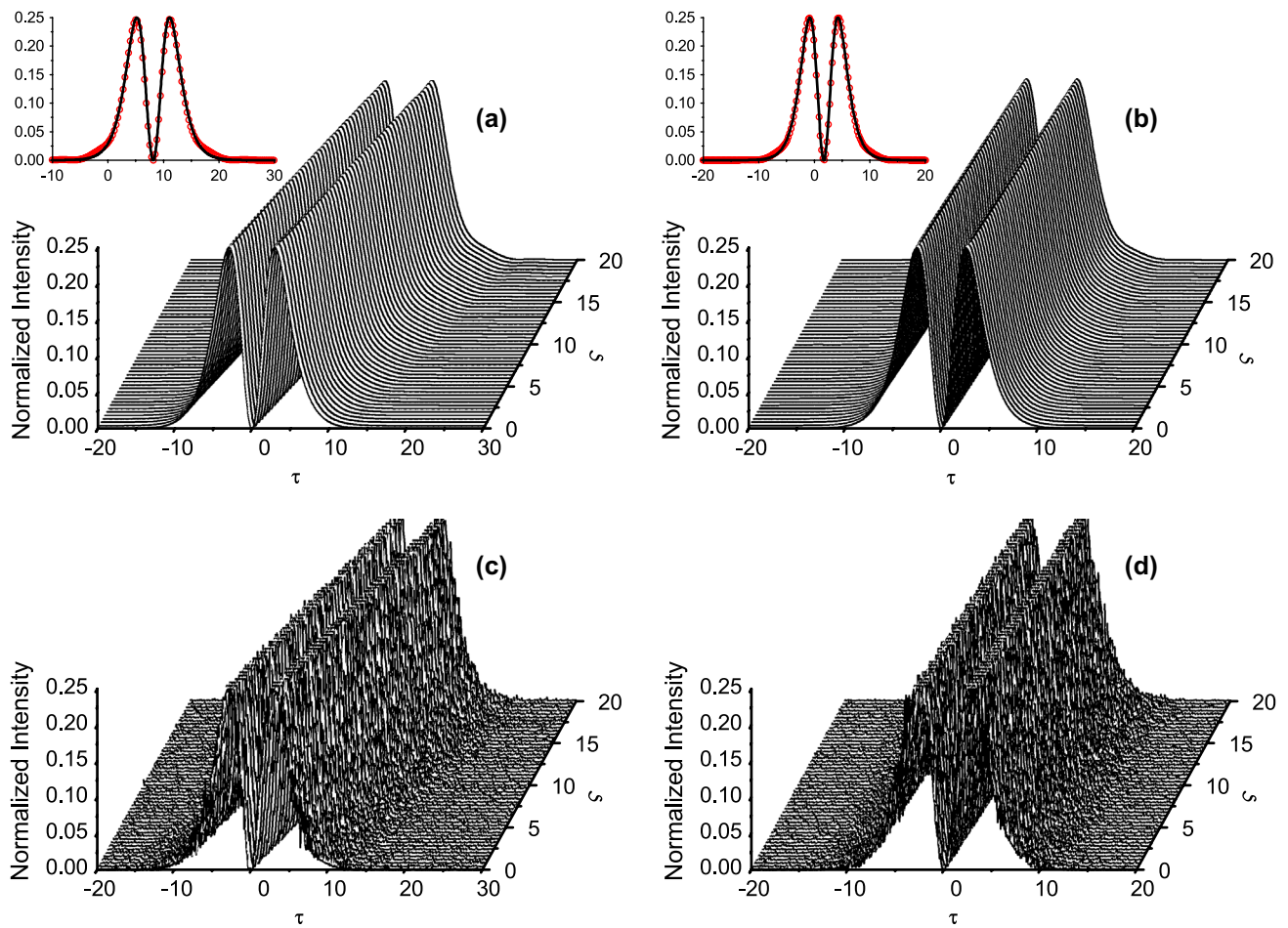


**Figure 4.** Numerical evolutions of the solitary wave (4) under (a) 5% pulse width fluctuation and (c) 10% random noise perturbation in normal-GVD regime of self-focusing negative-index MMs  $b_1 = 1$ ,  $b_2 = 1$  and  $\varpi = 0.777$  corresponding to  $b_3 = 12.014$  and  $b_4 = 24.506$ ; (b), (d) are those in anomalous-GVD regime of self-defocusing negative-index MMs  $b_1 = -1$ ,  $b_2 = -1$  and  $\varpi = 0.685$  corresponding to  $b_3 = 5.071$  and  $b_4 = -7.591$ , respectively. The insets in (a) and (b) show the comparisons of numerical simulation (red circle) and exact pulse (black solid line) after propagating 20 dispersion lengths.

### 3. Conclusion

In conclusion, we have considered a generalized NLSE with TOD and FOD for describing ultrashort pulse propagation in weakly nonlinear MMs, and an exact dipole solitary wave solution has been derived using an ansatz method. With reference to the Drude model, we have identified and discussed the existence regions of the new dipole solitary wave in MMs, which are much broader than those typically encountered in optical fibre systems. It has been found that the new wave can exist in normal-GVD regime of self-focusing negative-index MMs, in anomalous- and normal-GVD regimes of self-defocusing negative-index MMs, and in the anomalous-GVD regime of self-defocusing positive-index MMs. Furthermore, we have investigated the parameter variations of the solitary wave with normalized frequency in each existence region. The results show that Kerr nonlinearity only influences the existence regions, while GVD, TOD and FOD influence both the existence regions and the characteristics of

the solitary wave. The propagation properties can also be controlled by adjusting the frequency of incident waves. Finally, as examples, we investigated numerically the stability of the new dipole solitary wave in negative-index regimes involving normal-GVD with self-focusing nonlinearity, and anomalous-GVD with self-defocusing nonlinearity. The obtained results are useful for understanding how combined solitary wave dynamics and they might provide a basis for finding further novel forms of solitary waves in MMs.

### Disclosure statement

No potential conflict of interest was reported by the authors.

### Funding

This work was supported by the National Natural Science Foundation of China (NSFC) under [grant number 61178013], [grant number 61271160]; and Selected Project of Overseas

Science and Technology Activities of Shanxi Province under [Grant number 201301].

## References

- (1) Agrawal, G.P. *Nonlinear Fiber Optics*, 3rd ed.; Academic: San Diego, 2001.
- (2) Hasegawa, A.; Kodama, Y. *Solitons in Optical Communications*; Oxford University Press: Oxford, 1995.
- (3) Hasegawa, A.; Tappert, F. *Appl. Phys. Lett.* **1973**, *23*, 142–144.
- (4) Hasegawa, A.; Tappert, F. *Appl. Phys. Lett.* **1973**, *23*, 171–172.
- (5) Mollenauer, L.F.; Stolen, R.H.; Gordon, J.P. *Phys. Rev. Lett.* **1980**, *45*, 1095–1098.
- (6) Liu, W.J.; Tian, B.; Jian, Y.; Sun, K.; Qu, Q.X.; Li, M.; Wang, P. *J. Mod. Opt.* **2010**, *57*, 1498–1503.
- (7) Alka, X.G.; Goyal, A.; Gupta, R.; Kumar, C.N.; *Phys. Rev. A* **2011**, *84*, 063830.
- (8) Lin, X.G.; Liu, W.J.; Lei, M. *J. Mod. Opt.* **2015**, *62*, 658–661.
- (9) Li, Z.H.; Li, L.; Tian, H.P.; Zhou, G.S. *Phys. Rev. Lett.* **2000**, *84*, 4096–4099.
- (10) Yang, R.C.; Li, L.; Hao, R.Y.; Li, Z.H.; Zhou, G.S. *Phys. Rev. E* **2005**, *71*, 036616.
- (11) Hong, W.P. *Opt. Commun.* **2001**, *194*, 217–223.
- (12) Azzouzi, F.; Triki, H.; Mezghiche, K.; Akrimi, A.E. *Chaos Solitons Fractals* **2009**, *39*, 1304–1307.
- (13) Tian, J.P.; Tian, H.P.; Li, Z.H. *Phys. Scr.* **2003**, *7*, 325–328.
- (14) Choudhuri, A.; Porsezian, K. *Opt. Commun.* **2012**, *285*, 364–367.
- (15) Triki, H.; Azzouzi, F.; Grelu, P. *Opt. Commun.* **2013**, *309*, 71–79.
- (16) Lazarides, N.; Tsironis, G.P. *Phys. Rev. E* **2005**, *71*, 036614.
- (17) Scalora, M.; Syrchin, M.S.; Akozbek, N.; Poliakov, E.Y.; Aguanno, G.D.; Mattiucci, N.; Bloemer, M.J.; Zheltikov, A.M. *Phys. Rev. Lett.* **2005**, *95*, 013902.
- (18) Wen, S.C.; Xiang, Y.J.; Dai, X.Y.; Tang, Z.X.; Su, W.H.; Fan, D.Y. *Phys. Rev. A* **2007**, *75*, 033815.
- (19) Li, P.G.; Yang, R.C.; Xu, Z.Y. *Phys. Rev. E* **2010**, *82*, 046603.
- (20) Wen, S.C.; Xiang, Y.J.; Su, W.H.; Hu, Y.H.; Fu, X.Q.; Fan, D.Y. *Opt. Express* **2006**, *14*, 1568–1575.
- (21) Biswas, A.; Mirzazadeh, M.; Savescu, M.; Milovic, D.; Khan, K.R.; Mahmood, F.M.; Belic, M. Singular Solitons in Optical Metamaterials by Ansatz Method and Simplest Equation Approach. *J. Mod. Opt.* **2014**, *61*, 1550–1555.
- (22) Xiang, Y.J.; Wen, S.C.; Dai, X.Y.; Tang, Z.X.; Su, Z.X.; Fan, D.Y. *J. Opt. Soc. Am. B* **2007**, *24*, 3058–3063.
- (23) Latchio Tiofack, C.G.; Mohamadou, A.; Alim; Porsezian, K.; Kofane, T.C. Modulational Instability in Metamaterials with Saturable Nonlinearity and Higher-order Dispersion. *J. Mod. Opt.* **2012**, *59*, 972–979.
- (24) Marklund, M.; Shukla, P.K.; Stenflo, L. *Phys. Rev. E* **2006**, *73*, 037601.
- (25) Aguanno, D.; Mattiucci, N.; Scalora, M.; Bloemer, M.J. *Phys. Rev. Lett.* **2004**, *93*, 213902.
- (26) Tsitsas, N.L.; Rompotis, N.; Kourakis, I.; Kevrekidis, P.G.; Frantzeskakis, D.J. *Phys. Rev. E* **2009**, *79*, 037601.
- (27) Zhang, S.W.; Yi, L. *Phys. Rev. E* **2008**, *78*, 026602.
- (28) Boardman, A.D.; Mitchell-Thomas, R.C.; King, N.J.; Rapoport, Y.G. *Opt. Commun.* **2010**, *283*, 1585–1597.
- (29) Yang, R.C.; Zhang, Y. *J. Opt. Soc. Am. B* **2011**, *28*, ss123–127.
- (30) Shalaev, V.M. *Nat. Photonics* **2007**, *1*, 41–48.
- (31) Gunnar, D.; Christian, E.; Martin, W. *Opt. Lett.* **2006**, *31*, 1800–1802.
- (32) Alexander, K.P.; Vladimir, M.S. *Opt. Lett.* **2006**, *31*, 2169–2171.